

Electronic Supporting Information

Silica Nanoparticle Conjugation with Gallic Acid Towards Enhanced Free Radical Scavenging Capacity and Activity on Osteosarcoma Cells *in vitro*

*Mariam Hohagen,^a Nuno Saraiva^b Hanspeter Kählig,^c Christopher Gerner^d, Giorgia Del Favero,^{*e} Freddy Kleitz,^{*a}*

^a Department of Functional Materials and Catalysis, Faculty of Chemistry, University of Vienna, Währinger Straße 42, 1090 Vienna, Austria

^b CBIOS—Universidade Lusófona's Research Center for Biosciences & Health Technologies, Campo Grande 376, 1749-024 Lisbon, Portugal

^c Department of Organic Chemistry, Faculty of Chemistry, University of Vienna, Währinger Straße 38, 1090 Vienna, Austria

^d Department of Analytical Chemistry, Faculty of Chemistry, University of Vienna, Währinger Straße 38, 1090 Vienna, Austria

^e Department of Food Chemistry and Toxicology, Faculty of Chemistry, University of Vienna, Währinger Straße 38–40, 1090 Vienna, Austria

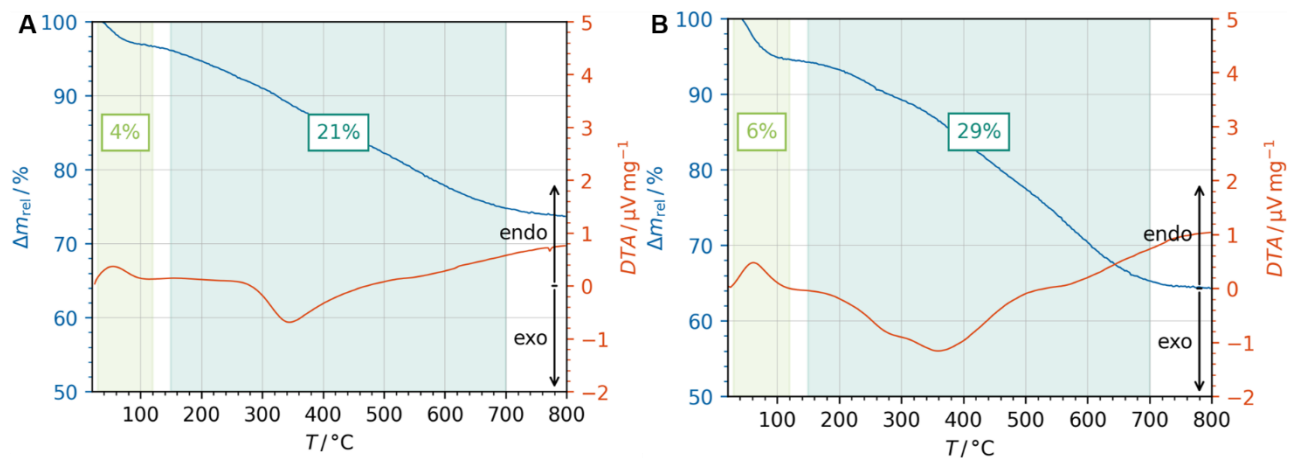


Figure S1. Coupled thermogravimetric analysis (TGA) and differential thermal analysis (DTA) of DMSNs conjugated with GA: DMSN-NCO-GA (A), and DMSN-NH-GA (B). The mass loss (blue line) was determined from 150 $^\circ\text{C}$ to 700 $^\circ\text{C}$ (dark green area) to exclude contributions from remaining solvents or water (light green area).

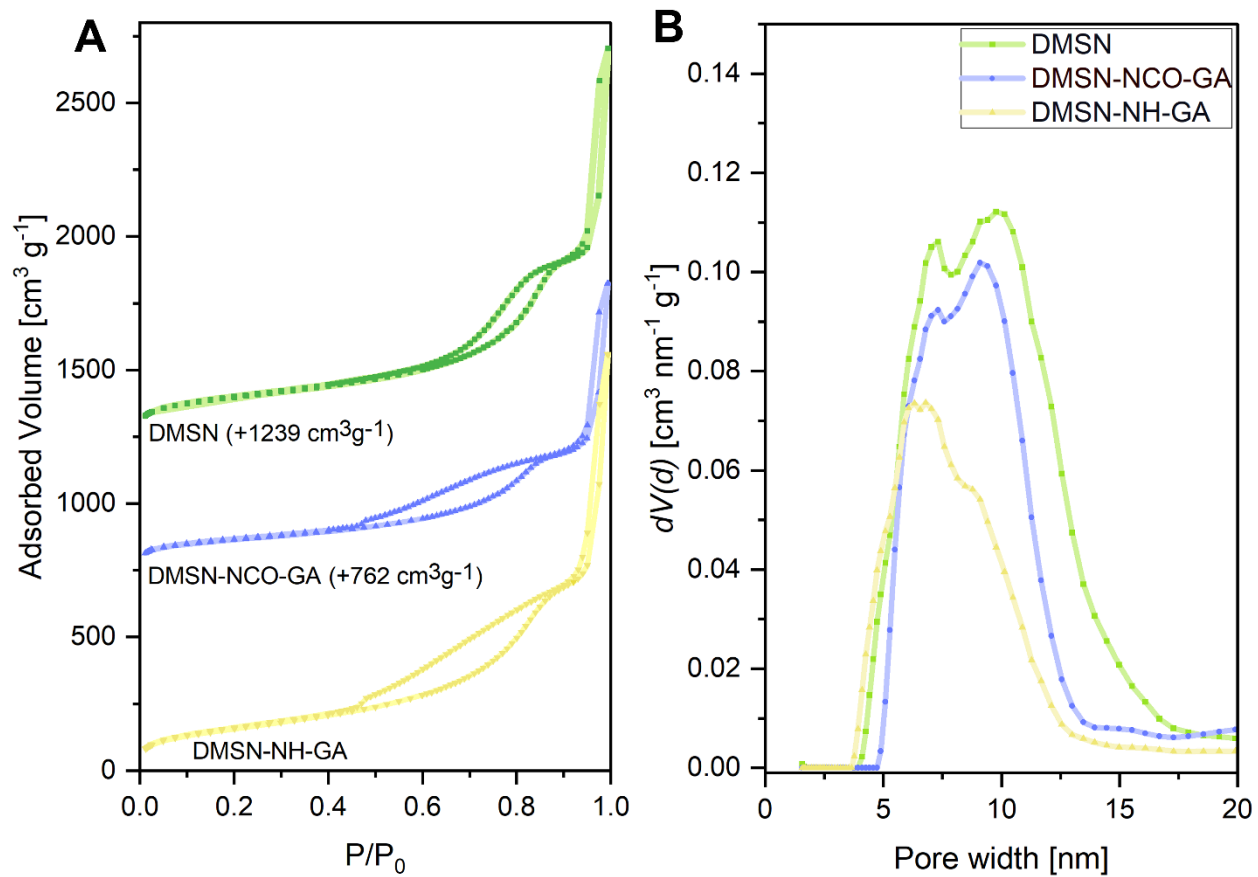


Figure S2. N₂ physisorption isotherms (measured at - 196 °C) of the different DMSNs, as indicated, (A) and their respective NLDFT pore size distributions (B).

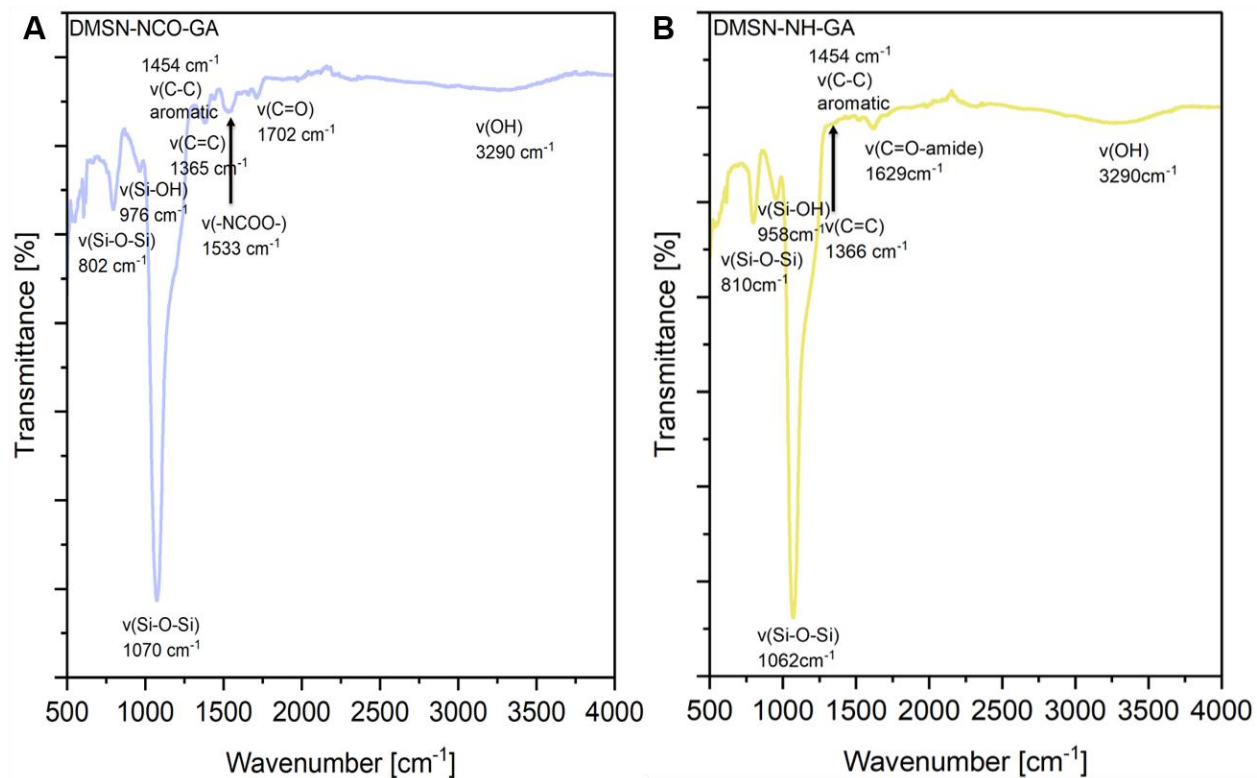


Figure S3. Attenuated total reflectance infrared (ATR-IR) spectra of GA-functionalized DMSNs: DMSN-NCO-GA (A), and DMSN-NH-GA(B).

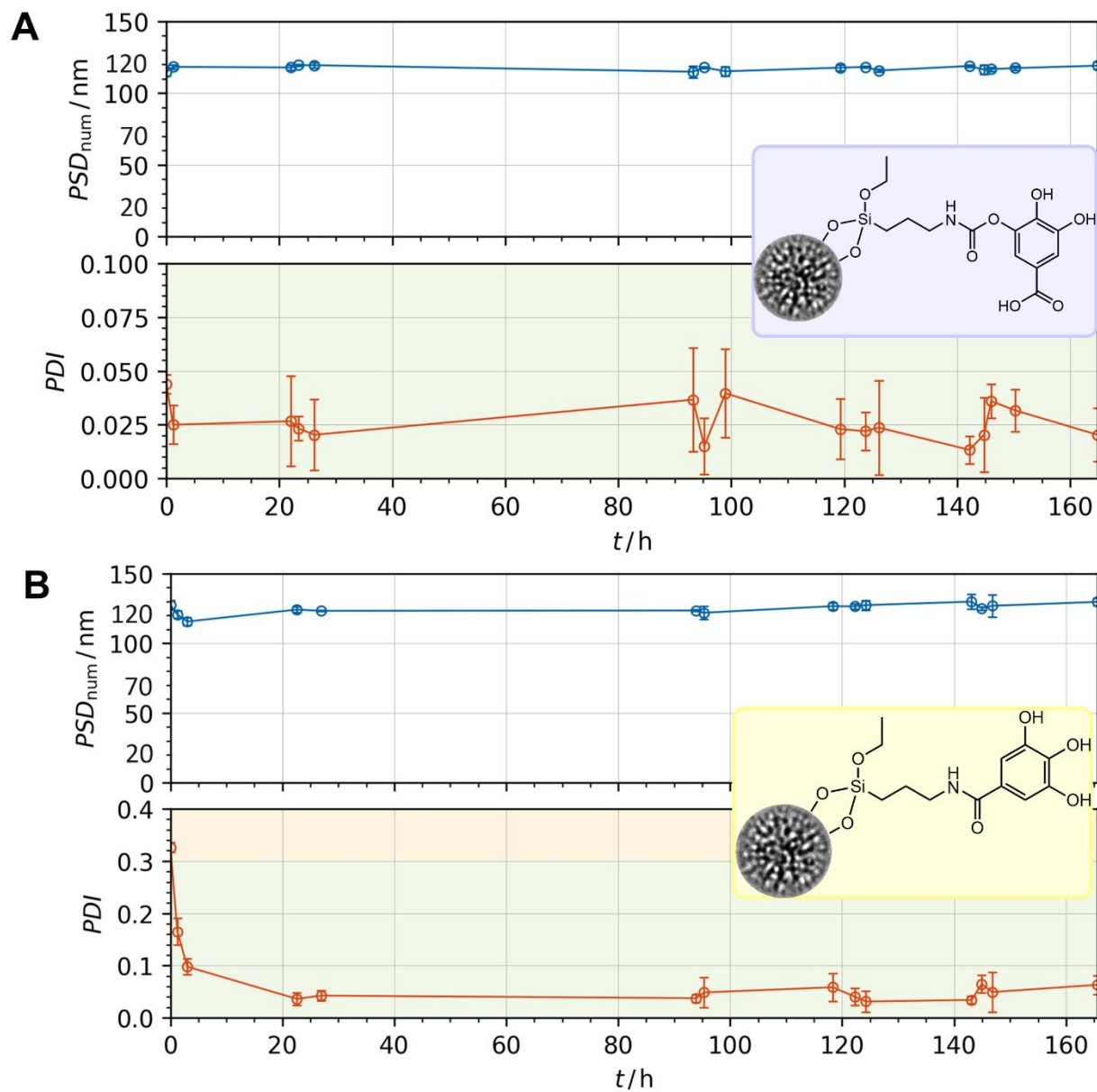


Figure S4. Colloidal stability tests via dynamic light scattering (DLS) measurements of DMSN-NCO-GA (A), and DMSN-NH-GA (B).

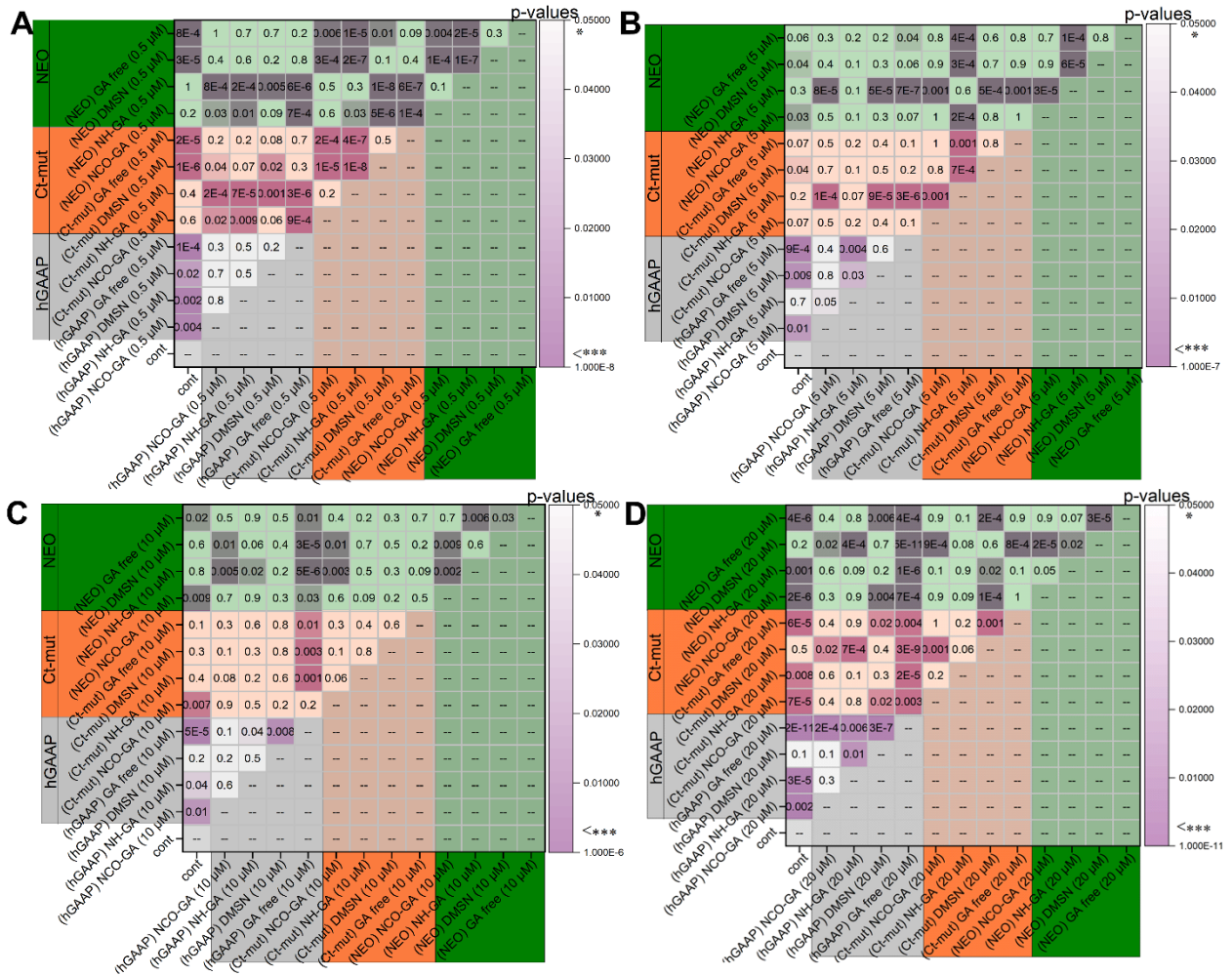


Figure S5. Statistical evaluation of the cell viability assay in the presence of GA-conjugated particles as measured by metabolic activity (cell titer blue assay) in U2-OS cell lines (hGAAP (grey), NEO (orange), and Ct-mut (green)) after incubation for 24 h. The difference among the treatments was determined via one-way ANOVA with Fisher LSD (* $p < 0.05$; ** $p < 0.01$; *** $p < 0.001$, depicted in violet).

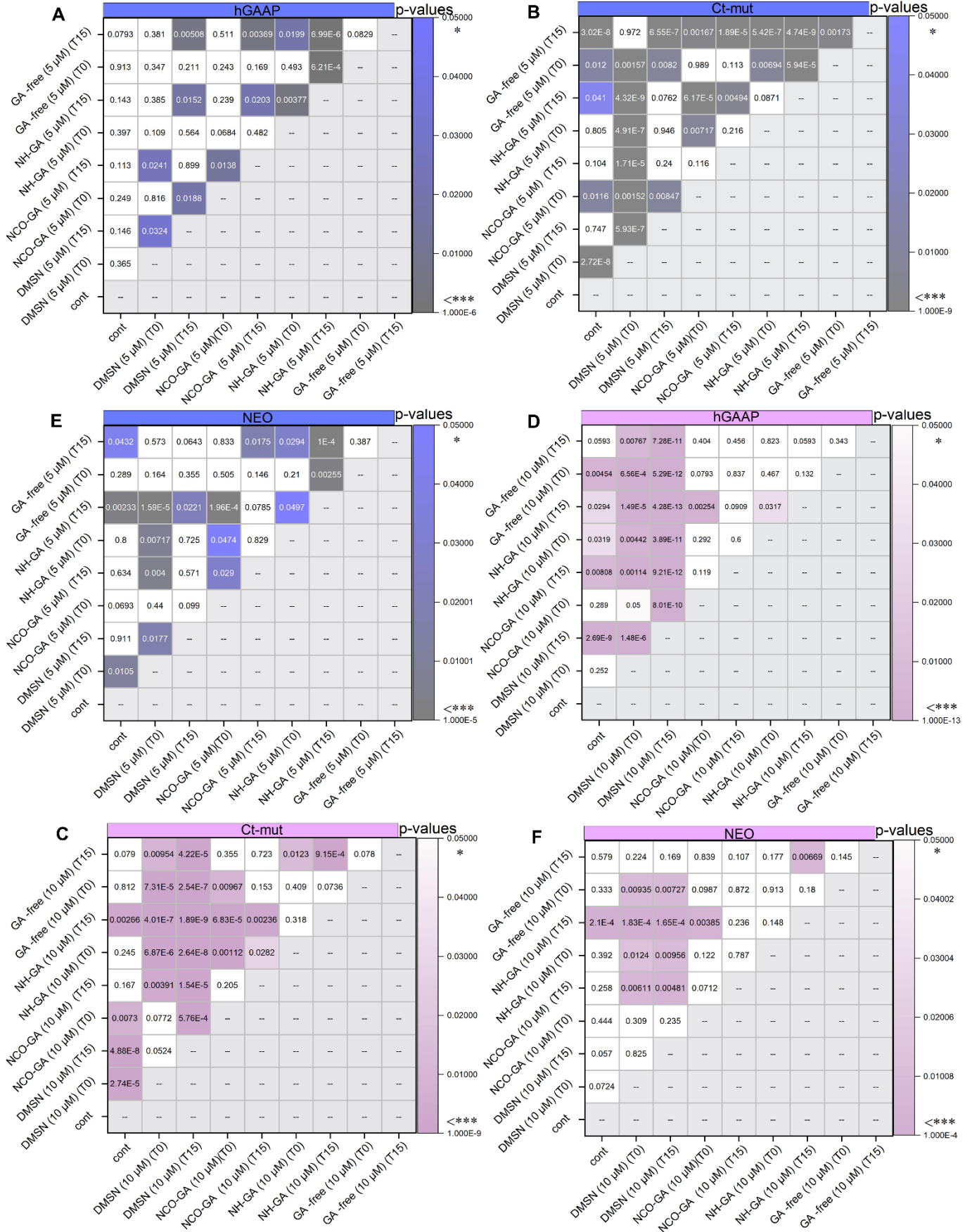


Figure S6. Statistical analysis was performed on the signal intensity quantification after incubating U2-OS cell lines (hGAAP (A, D), Ct-mut (B, E), and NEO (C, F)) with free GA, DMSN-NH-GA, and DMSN-NCO-GA, in the absence of an oxidative stressor. The incubation was performed for 24 h with a GA concentration of 5 μM (A-C) and 10 μM (D-F), and non-functionalized DMSNs with concentrations equivalent to 5 μM and 10 μM GA, namely 53.15 $\mu\text{g mL}^{-1}$ and 106.3 $\mu\text{g mL}^{-1}$. Three independent cell preparations were conducted, and the data was expressed as an average fluorescence intensity normalized to the relative fluorescence generated by the application of the solvent control. The difference among the treatments was assessed using one-way ANOVA with Fisher LSD (* $p < 0.05$; ** $p < 0.01$; *** $p < 0.001$, depicted in grey to blue and violet).

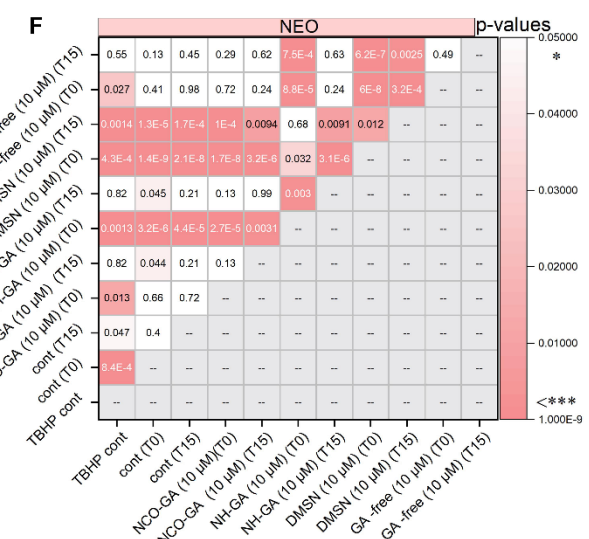
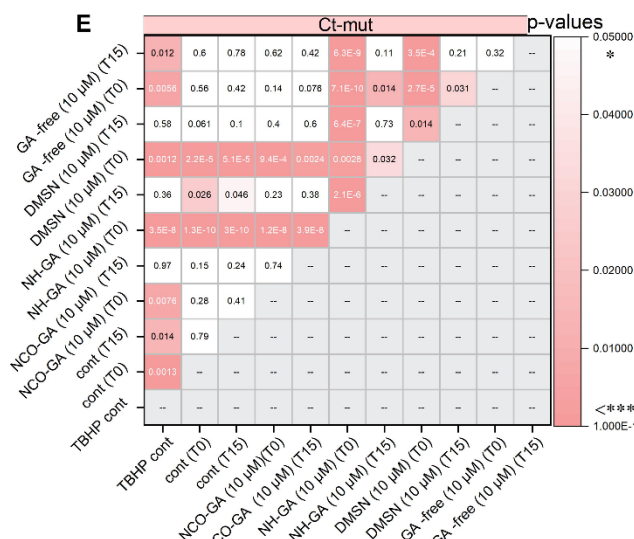
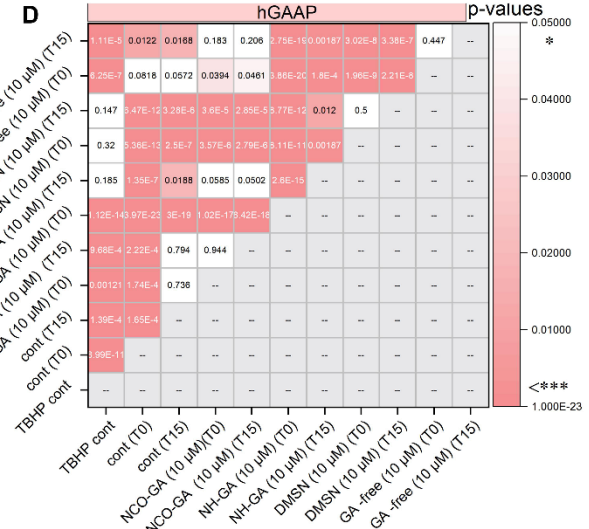
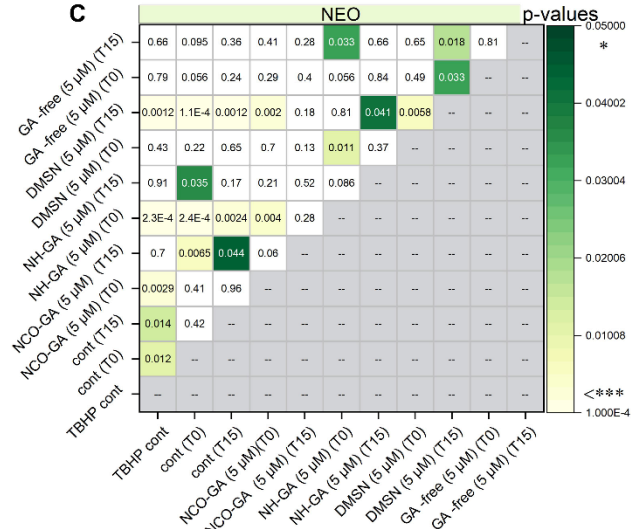
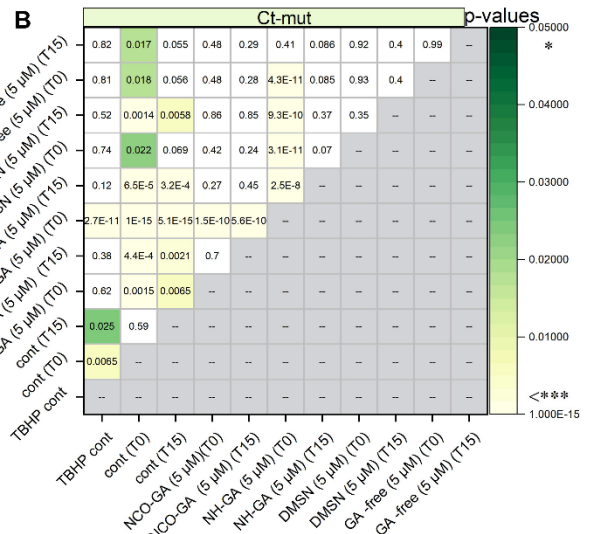
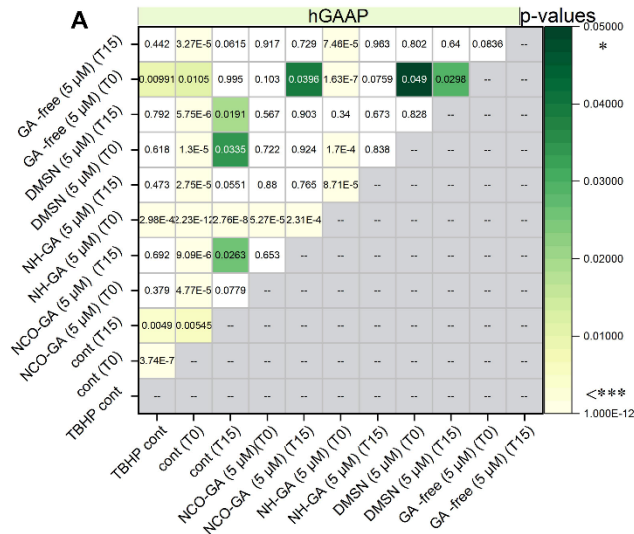


Figure S7. Statistical analysis was conducted on the signal intensity quantification after incubating U2-OS cell lines (hGAAP (A, D), Ct-mut (B, E), and NEO (C, F)) with free GA, DMSN-NH-GA, and DMSN-NCO-GA, in the presence of TBHP (0.2 mM) as an oxidative stressor at GA concentration of 5 μ M (A-C) and 10 μ M (D-F). Additionally, non-functionalized DMSNs were used at concentrations equivalent to 5 μ M and 10 μ M GA, corresponding to 53.15 μ g mL⁻¹ and 106.3 μ g mL⁻¹. Three independent cell preparations were conducted, and the data was expressed as the average fluorescence intensity normalized to the relative fluorescence triggered by TBHP. The difference among the treatments was assessed using one-way ANOVA with Fisher LSD (* p < 0.05; ** p < 0.01; *** p < 0.001, depicted in green to yellow and red to pink).

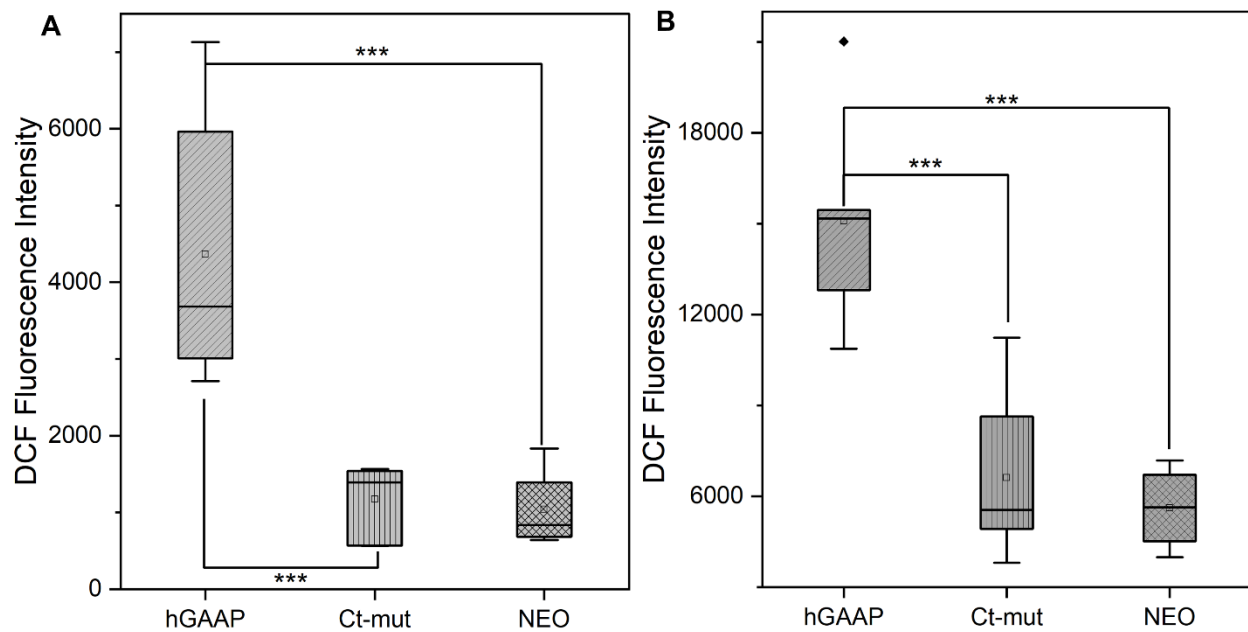


Figure S8. Baseline of DCF fluorescence intensity measured at t = 0 (A) and t = 15 min (B) after treatment with an oxidative stressor TBHP (0.2 μ M). The data was collected from n = 16, with measurements conducted in technical triplicates. The difference among TBHP treatment was determined using one-way ANOVA with Fisher LSD (* p < 0.05; ** p < 0.01; *** p < 0.001).

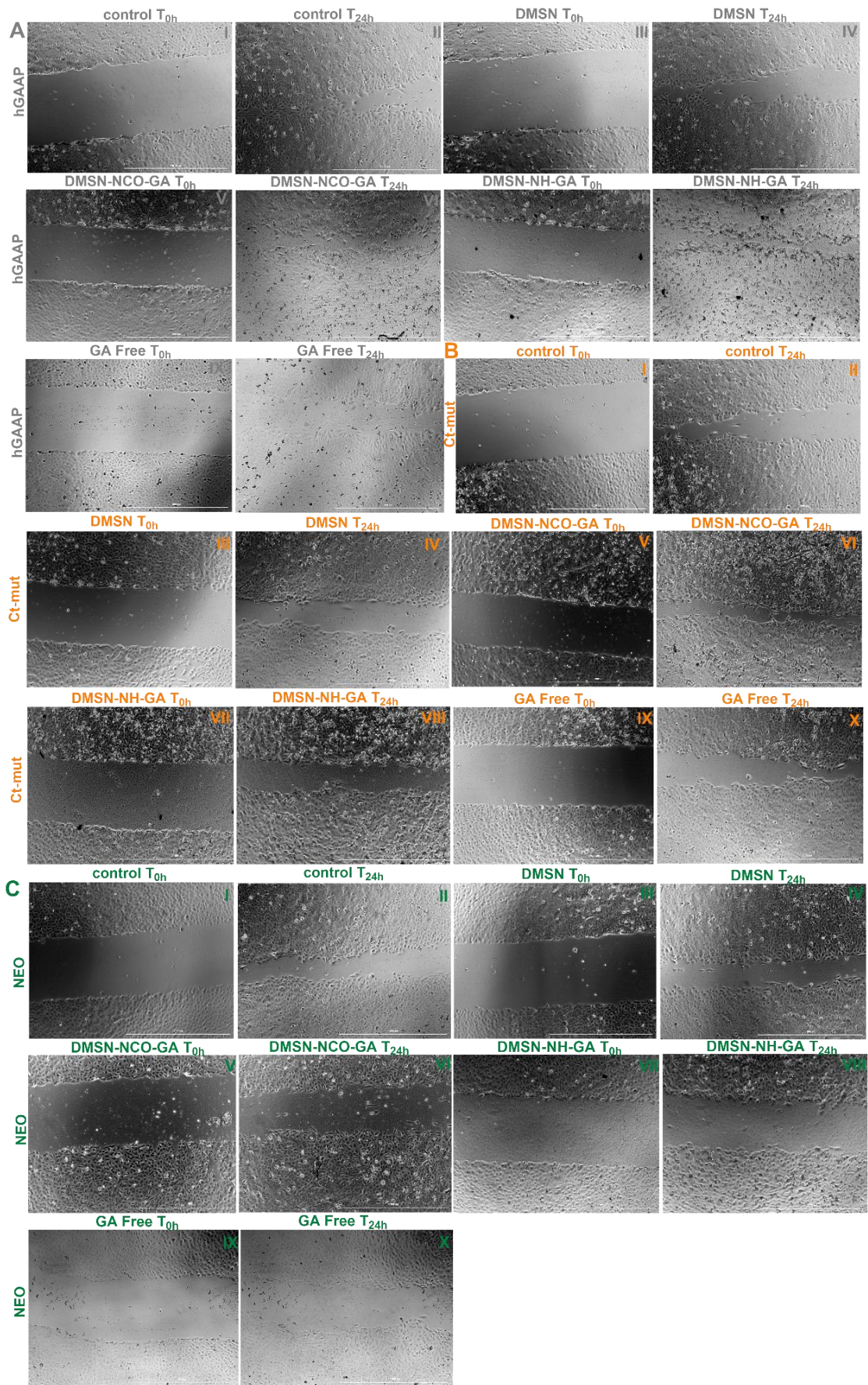


Figure S9. Representative phase contrast images acquired during the migration assays and depicting the beginning ($t = 0$) and the end of the assay ($t = 24$ h). scale bar: 1000 μm).

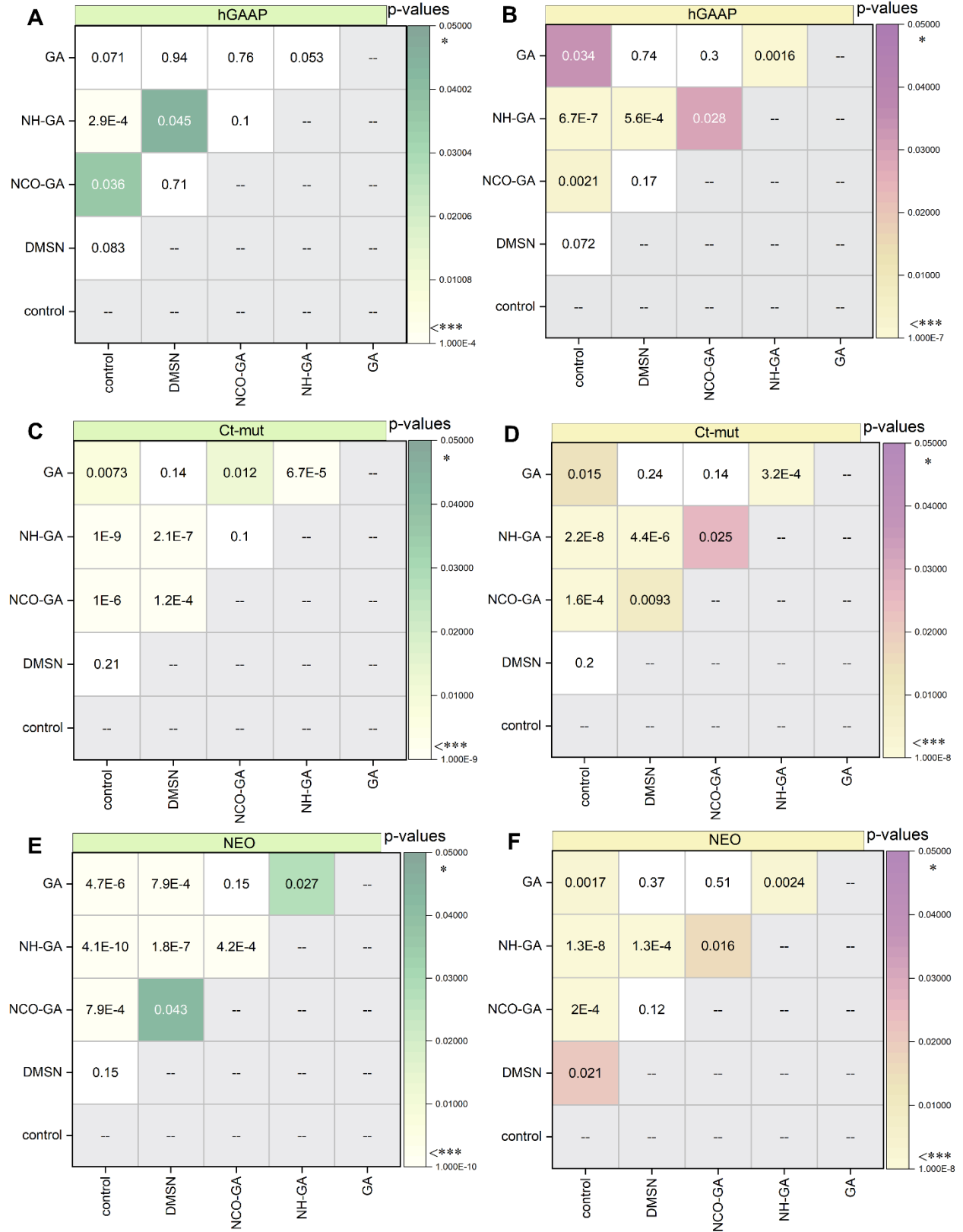


Figure S10. Statistical assessment of migration changes in U2-OS cell lines (hGAAP (A, B), Ct-mut (C, D), and NEO (E, F)) was conducted following incubation with GA-conjugated materials, and free GA at a GA concentration of 10 μM . Additionally, non-functionalized DMSNs were used at concentrations equivalent to 10 μM GA, corresponding to 106.3 $\mu\text{g mL}^{-1}$. The evaluation comprised two aspects: firstly, the area grown [μm^2] was determined by calculating the difference between the initial scratch area and the area at the same coordinates after 24 h of incubation (n =16) (A, C, and E). Secondly, the closure velocity ($\mu\text{m h}^{-1}$) was computed as the difference between the initial and final gap distances at the same coordinates, divided by the overall time (24 h) in untreated control, non-functionalized DMSNs, and GA-conjugated materials treated cells (B, D, and F). The difference among treatment groups was assessed using one-way ANOVA with Fisher LSD (* p < 0.05; ** p < 0.01; *** p < 0.001, represented by color variations green to yellow or pink to yellow).